

Research Journal of Pharmaceutical, Biological and Chemical Sciences

Bio-Impedance Analysis for Classification of Various Skin Diseases in Indian Context.

Durgaprasad K Kamat^{1*}, and Pradeep M Patil².

¹Sinhgad College of Engineering, Pune, India.

²Jayawantrao Sawant College of Engineering, Pune, India

ABSTRACT

This paper describes a non-invasive embedded healthcare system using bio-impedance analysis and Modular Fuzzy Hypersphere Neural Network (MFHSNN) with its learning algorithm, proposed by P. Patil et al [1] for identification and classification of various skin diseases. Bio-impedance analysis has potential to discriminate between the diseased and normal skin. Various electrical impedance indices like magnitude index (MIX), phase index (PIX), real-part index (RIX) and imaginary-part index (IMIX) have been computed for diseased and normal skin. Statistical parameters of these indices, along with their individual values, have been used as the features of diseased skin and applied to MFHSNN for further classification. Each module in MFHSNN is exposed to patterns of only one class and trained without overlap test and removal, as MFHSNN offers higher degree of parallelism, leading to reduction in training time and captures peculiarity of only one particular class. Hence, it is used to classify facial melanoses, acne vulgaris, folliculitis and tineacorporis skin diseases, where new patterns can be added on fly. The MFHSNN is found superior in terms of generalization and training time with equivalent testing time.

Keywords: Bio-impedance, Modular Fuzzy Hypersphere Neural Network, non-invasive, embedded healthcare system, skin diseases.

**Corresponding author*

INTRODUCTION

Bio-impedance is the opposition by human body to an alternating current flow. A good bio-impedance measurement requires sweep of frequency over a wide range. Bio-impedance measurement and analysis is an evolving area of research; though many researchers have contributed a lot in terms of developing new measurement techniques for analysis of various diseases. The bio-impedance research domain publications in refereed Journals and Transactions are exponentially growing during last three decades. Bio-impedance measurements have been used as a tool to discriminate between diseased and normal skin. Electrical impedance measurement of the skin tissue proves to be a non-invasive, reliable, simple, safe and objective technique.

Electrical bio-impedance has been used to assess skin cancers and other cutaneous lesions. The different types of skin cancer like malignant melanoma, basal cell carcinoma and squamous cell carcinoma have been analyzed using bio-impedance measurements. P. Aberg et al [2] have distinguished skin cancer from benign nevi using multi-frequency impedance spectra. The impedance relation between lesion and reference skin was used to distinguish the cancers from the nevi. The electrical impedance measurements have been used by I. Nicander et al [3] to discriminate between the effects of different irritant substances upon the human skin. The magnitude and phase of electrical impedance were measured and four impedance indices namely magnitude index (MIX), phase index (PIX), real-part index (RIX) and imaginary-part index (IMIX), were devised from the impedance data for statistical analysis. The electrical impedance method has been used by L. Emtestam et al [4] for preoperative assessment of nodular basal cell carcinoma (BCC). The results suggested that BCC can be investigated using electrical impedance measurement. The diagnostic potential of electrical impedance to discriminate BCC with reference to benign tumors and normal skin has been identified by D. Beetner et al [5]. The impedance indices have shown smaller values for BCC than for benign lesions or normal skin. T. Uchiyama et al [6] have conducted bioelectrical impedance analysis (BIA) for skin rubor and intact skin to identify skin rubor. Modeling approach has been used by S. Koppa et al [7] to study the effects of the electrode placement in tetra-polar bio-impedance measurements at the surface of the skin.

Pattern recognition applications widely use fuzzy neural networks. Many papers using fuzzy neural networks have been reported on studies of pattern classification and clustering. Kwan et al [8] have proposed four-layer feed forward unsupervised fuzzy neural network (FNN). U. Kulkarni et al [9] modified FNN to work under supervised environment, which was further extended, by P. Patil et al [10] using selective aggregation operators. P. Patil et al [11] also implemented GFHLSNN for generalization.

In present work, non-invasive portable embedded healthcare system has been used for bio-impedance measurements of skin diseases namely facial melanoses, acne vulgaris, folliculitis and tineacorporis. Facial melanoses cause cosmetic disfigurement in patients and common skin disease in India. [12]. Acne vulgaris is a chronic inflammatory disease of pilosebaceous units, mainly affecting adolescent population [13]. Folliculitis is the presence of inflammatory cells within the wall and ostia of human hair follicle, creating a follicular-based pustule[14]. Tineacorporis is an infection by dermatophytes fungi that invade and multiply within skin, hair and nails [15].

The bio-impedance analysis of skin diseases involves computation of four indices namely magnitude index (MIX), phase index (PIX), real-part index (RIX) and imaginary-part index (IMIX).Statistical features of these indices have been computed by using mean and standard deviation. Box and whisker plot provides the descriptive statistics of the computed indices. Significant differences for the indices have been computed using Wilcoxon signed rank test and help in discrimination between diseased and normal skin. The purpose of this work is twofold. Initially, we prove that bio-impedance has a potential to discriminate between diseased and normal skin for diseases namely facial melanoses, acne vulgaris, folliculitis and tineacorporis; followed by classification of the said skin diseases based on MFHSNN. In order to classify these diseases, we have implemented the MFHSNN algorithm [1] and used this algorithm for identification and classification of various skin diseases. Performance of the proposed system has been validated with the histopathological examination by the experts.

This paper is organized as follows. Block diagram of the proposed system for identification of the skin diseases is explained in Section II. Generation of skin disease database using embedded healthcare system is described in Section III. The significant differences between diseased and normal skin have been elaborated in

Section IV. Classification of skin diseases using MFHSNN has been presented in Section V. Results and discussions are stated in Section VI.

PROPOSED SYSTEM

The block diagram of proposed system for analysis of various skin diseases, namely facial melanoses, acne vulgaris, lichen planus and tinea corporis, is shown in Figure 1. The system consists of skin electrode, impedance converter, microcontroller and personal computer. The skin impedance is measured by attaching the electrode to the skin. The impedance converter IC AD5933 measures the real and imaginary parts of complex impedance of human skin. Cypress microcontroller CY7C68013A computes impedance with the help of real and imaginary values, read from impedance converter. The personal computer reads impedance data from microcontroller and stores in database for further analysis. The individual blocks are explained in detail in the following section.



Figure (2): Developed skin electrode.

Skin electrode

The impedance of human skin is measured with the help of a developed skin electrode as shown in Figure 2. The electrode is fabricated using glass epoxy material and coated with Ag/AgCl material. The skin electrode consists of two concentric electrodes; outer source and inner sink electrode. The size of source and sink electrode is based on effective impedance measurement of diseased skin. The outer source electrode is connected to the V_{out} pin; while the inner sink electrode is connected to the V_{in} pin of AD5933. The insulating guard band between source and sink electrodes reduces effects of surface currents. The inner circular sink electrode is approximately 10 mm in diameter, as majority of skin lesions in our experimentation were larger than 10 mm in size. The outer source electrode applies alternating current to the skin lesions; while the inner sink electrode measures the response signal from the skin lesions.

Impedance converter IC AD5933

The IC AD5933 is known for high precision impedance converter system. It has an on-board frequency generator combined with a 12-bit, 1 MSPS ADC. The complex impedance to be measured is excited by known frequency with the help of frequency generator. At each excitation frequency, on-board DSP engine computes DFT taking sampled response signal from the impedance to be measured. The sampling is performed by the on-board ADC. The entire board is powered by USB port connected to a computer. The I2C signals generated by USB microcontroller are used as an interface to AD5933. The USB microcontroller connects to Visual basic graphic user interface that runs on computer [16].

Microcontroller IC CY7C68013A

The microcontroller IC CY7C68013A is interfaced to AD5933 on the evaluation board AD5933EBZ. The microcontroller reads impedance data from impedance converter. It acts as a programmable interface between impedance converter and personal computer for database generation. The microcontroller IC CY7C68013A has a single-chip integrated USB 2.0 transceiver, smart serial interface engine (SIE) and enhanced 8051 microprocessor. It is ultra-low power IC, ideal for bus- and battery-powered applications. It supports 8051 software code that runs from internal RAM, downloaded through USB [17].

Personal computer

The personal computer has been used to generate bio-impedance database. The personal computer runs visual basic front-end program that has been bundled with the AD5933EBZ evaluation board. The impedance of diseased and normal human skin, at 20 kHz and 500 kHz, has been measured using AD5933. The impedance database has been downloaded onto personal computer. The impedance indices were computed and stored in the database. Statistical analysis of impedance indices was performed using Statistical Package for Social Sciences (SPSS) to calculate mean, standard deviation and to plot box and whisker plots. The classifier MFHSNN classifies the skin diseases into four class, namely facial melanoses (C_1), acne vulgaris (C_2), folliculitis (C_3) and tineacorporis(C_4).

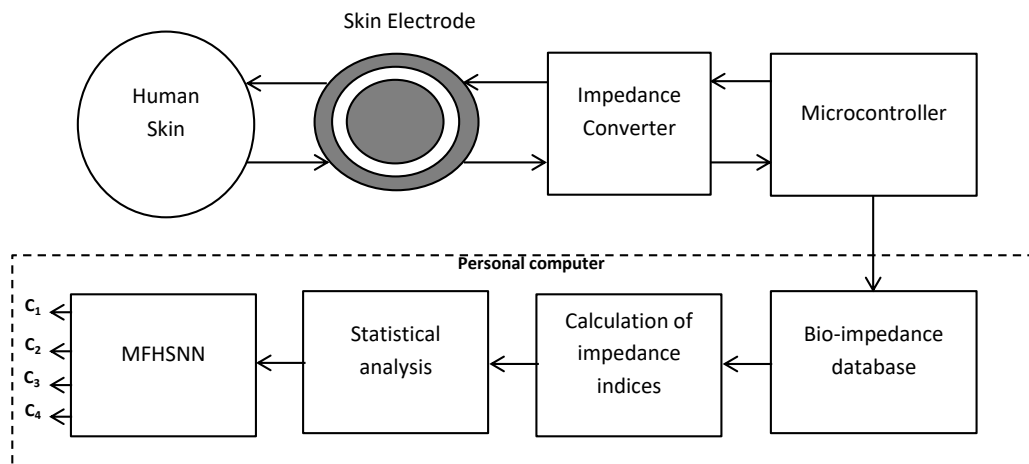


Figure (1): Block diagram to generate database of various skin diseases using bio-impedance analysis.

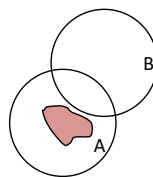


Figure (3): Electrode positions for skin impedance measurement, (a) with lesion at the center of the measurement electrode and (b) with the electrode placed on normal skin immediately adjacent to the lesion

DATABASE GENERATION

Electrical impedance of diseased and normal skin was measured in vivo at 20 kHz and 500 kHz. Measurements were carried out with Analog Devices board AD5933EBZ. The bio-impedance measurements were performed for facial melanoses, acne vulgaris, folliculitis and tineacorporis skin diseases. Our in-house generated dataset included 24 lesions for facial melanoses, 29 for acne vulgaris, 37 for folliculitis and 18 for tineacorporis. Impedance of normal skin adjacent to lesions was measured for all these 108 locations. The basic measurement positions are shown in Figure 3.

The lesions available for in this work were of different sizes. The lesions, best fitting the size of electrode, were chosen for measurement so as to avoid inclusion of normal skin in impedance measurement of lesion, and to get accurate measurement results. The various skin diseases were confirmed following the medical procedures of Smt. KashibaiNavale Hospital located at Narhe (Bk), Pune, Maharashtra state, India and Bharti Hospital located at Dhankawadi, Pune, Maharashtra state, India.

STATISTICAL ANALYSIS

The bio-impedance analysis of the said skin diseases has been carried out, for each measurement, in terms of various indices, based on magnitude (MIX), phase (PIX), real-part (RIX) and imaginary-part (IMIX) of skin impedance. The impedance indices are defined as follows [3].

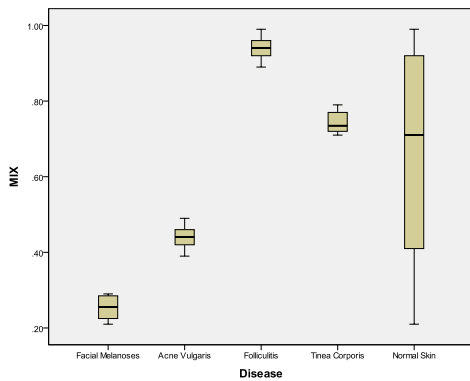
$$MIX = \frac{abs(Z_2)}{abs(Z_5)}$$

$$PIX = \arg(Z_{20}) - \arg(Z_{500}) \tag{1}$$

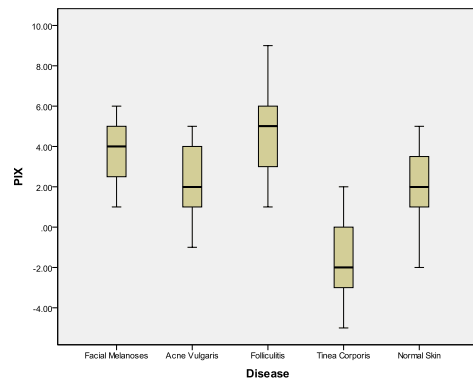
$$RIX = \frac{Re(Z_{20})}{abs(Z_{500})} \tag{2}$$

$$IMIX = \frac{Im(Z_{20})}{abs(Z_{500})} \tag{3}$$

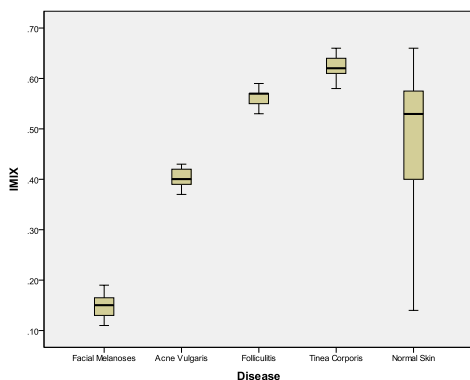
(4)



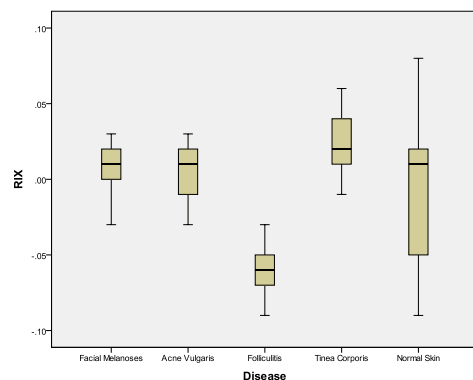
(a)



(b)



(c)



(d)

Figure (4): Box and whisker plots for the four indices of facial melanoses, acne vulgaris, folliculitis and tinea corporis skin diseases and normal skin (a) MIX, (b) PIX, (c) IMIX and (d) RIX.

where,

- $abs(Z_i)$ is magnitude (modulus) of the complex electrical impedance at frequency i ,
- $arg(Z_i)$ is argument (phase angle) of the complex electrical impedance at frequency i in degrees,
- $Re(Z_i)$ is real part of the complex electrical impedance at frequency i ,
- $Im(Z_i)$ is imaginary part of the complex electrical impedance at frequency i .

It has been observed that the accuracy of measurement is subject to the size of the measurement electrode; as lesions under measurement were of different shapes and sizes. If the size of lesion beneath the measurement electrode matches the size of electrode, measurements are accurate. The values of MIX, PIX, IMIX and RIX for various skin diseases were computed and recorded in the database.

It has been observed that one cannot predict the type of disease and the difference between the normal and diseased skin only with the help of measured electrical bio-impedance but can conclude partially from the relationship between computed values of the indices. The hypothesis to identify the difference between diseased and normal skin, based on various indices, has been tested using the Wilcoxon signed rank test.

In our study, depth of measurement was not considered as a parameter during the experimentation because it does not have significant effect on the results [5]. Measured values of MIX, PIX, RIX and IMIX of facial melanoses, acne vulgaris, folliculitis and tineacorporis skin diseases and normal skin are shown in Figure 4, with the help of box and whisker plots for the four indices. The median value of dataset is represented by a line in the middle of each box. The boxes extend above and below the median to include 25% of the measured data points in each direction. Whiskers extend to the minimum and maximum measured value. Various skin diseases form the X-axis and various indices are depicted on Y-axis. Measurements at the surface of diseased and normal skin, for each of the subjects, are included for the said diseases.

TABLE 1: MEAN AND STANDARD DEVIATION OF VARIOUS INDICES

Index	Measurement for	Mean ± Standard Deviation
MIX	Facial Melanoses	0.2525±0.02923
	Acne Vulgaris	0.4393±0.02815
	Folliculitis	0.9416±0.02598
	TineaCorporis	0.7533±0.04911
	Normal Skin	1.1736±0.0507
PIX	Facial Melanoses	4.4583±0.97709
	Acne Vulgaris	2.5862±1.05279
	Folliculitis	4.5946±1.01268
	TineaCorporis	-0.8889±1.18266
	Normal Skin	2.1852±1.7938
IMIX	Facial Melanoses	0.1479±0.0234
	Acne Vulgaris	0.4141±0.08555
	Folliculitis	0.563±0.02039
	TineaCorporis	0.6211±0.02564
	Normal Skin	0.8556±0.26789
RIX	Facial Melanoses	0.0075±0.018
	Acne Vulgaris	0.0069±0.01734
	Folliculitis	0.0541±0.03320
	TineaCorporis	0.0211±0.02026
	Normal Skin	-0.0513±0.02268

The mean and standard deviation values of various indices for the said diseases are summarized in Table 1. The mean value of MIX was lowest for facial melanoses and highest for folliculitis; while that for acne vulgaris and tineacorporis fall in between these two in increasing order. The mean value of MIX for normal skin was found to be highest for all the diseases. Based on the observed mean values of MIX, two groups of diseases can be clearly identified; facial melanoses and acne vulgaris with lower values; while folliculitis and tineacorporis having higher values of MIX. The mean value of PIX was found to be lowest for tineacorporis followed in increasing order by acne vulgaris, facial melanoses and folliculitis. Significant differences were not observed between facial melanoses and folliculitis in terms of PIX. Significant differences generally were not found, in terms of RIX, for all the four diseases. Values of IMIX were significantly lower for facial melanoses in comparison with acne vulgaris, folliculitis and tineacorporis. Amongst the later three, the values of IMIX were observed to follow an increasing trend.

Statistically significant differences between indices of diseased and normal skin were estimated using the Wilcoxon signed rank test. The probability of similarity between the indices (MIX, PIX, RIX and IMIX) of diseased and normal skin, for facial melanoses, acne vulgaris, folliculitis and tineacorporis skin diseases, has been computed using SPSS. When the probability of similarity is less than 0.05, distributions are said to be significantly different.

Probability of similarity between distributions of indices for diseased and normal skin is shown in Table 2. Significant differences have been observed between diseased and normal skin for MIX, PIX and IMIX values of facial melanoses, acne vulgaris, folliculitis and tineacorporis as the probability of similarity is far less than 0.05. In case of RIX, excepting the case of folliculitis, the distributions of all other diseases have shown significant differences. Hence, based on the significant differences, MIX, PIX and IMIX contribute towards the differentiation between diseased and normal skin. Excepting the case of folliculitis, RIX also contributes to differentiate between diseased and normal skin.

CLASSIFICATION USING MFHSNN

In this work, we have implemented four layer MFHSNN for classifying facial melanoses, acne vulgaris, folliculitis and tineacorporis skin diseases. During training phase, four modules of MFHSNN are used, since database consists of patterns of four classes of skin diseases. First two layer feed forward neural network grows adaptively to meet the demands of the problem. The first layer accepts n-dimensional input patterns selected as the statistical information of the indices, along with individual values of the indices, and the second layer consists of hyperspheres (HSs) that are created during training. In this work, we have used minimum value, first quartile, median, third quartile and maximum value of indices of a particular disease, along with MIX, PIX, IMIX and RIX of diseased and normal skin for individual subjects, as input features. Hence, the first layer has 13-dimensional input patterns, along with class label. Each module is trained with patterns of that skin disease class to which it represents. Hence, each module learns peculiarities of a single skin disease class.

TABLE 2: PROBABILITY OF SIMILARITY BETWEEN VARIOUS IMPEDANCE MEASURES

Index	Similarity between	Probability
MIX	Facial Melanoses& Normal Skin	0.0000179835
	Acne Vulgaris & Normal Skin	0.0000025288
	Folliculitis & Normal Skin	0.00000011
	TineaCorporis& Normal Skin	0.000189988
PIX	Facial Melanoses& Normal Skin	0.0082524531
	Acne Vulgaris & Normal Skin	0.0030399216
	Folliculitis & Normal Skin	0.0000001448
	TineaCorporis& Normal Skin	0.0075999592
IMIX	Facial Melanoses& Normal Skin	0.0000175793
	Acne Vulgaris & Normal Skin	0.0000025050
	Folliculitis & Normal Skin	0.0000001066
	TineaCorporis& Normal Skin	0.0001903234
RIX	Facial Melanoses& Normal Skin	0.0000638237
	Acne Vulgaris & Normal Skin	0.000004999
	Folliculitis & Normal Skin	0.1033675355
	TineaCorporis& Normal Skin	0.0001843516

The weights between first and second layer, for any k^{th} module, represent center points and radii of the HSs created during learning. These weights are stored in a matrix CP^k . Each row in CP^k is $(n + 1)$ dimensional vector in which first n components represent center point and $(n + 1)^{th}$ component contains radius of the HS. In this work, each row in CP^k is 14-dimensional vector with first 13 components relating to indices of diseased and normal skin of individual subjects and statistical parameters of indices of a particular disease. The 14th dimension represents radius of the HS. Each HS module is characterized by, a center point, radius and a fuzzy membership function. A value between 0 and 1 is returned by fuzzy membership function.

The processing is performed by j^{th} fuzzy HS node in k^{th} module, i.e. m_j^k . The threshold input of HS denoted as T is set to one and it is weighted by ζ_j^k , where ζ_j^k represents radius of HS m_j^k , which is updated during training. The maximum size of HS is bounded by a user defined value λ , called as growth parameter where $0 \leq \lambda \leq 1$. Hence, λ puts maximum limit on the radius of the HS.

Assuming the training set defined as $R = \{R_h | h = 1, 2, \dots, n\}$, where $R_h = (r_{h1}, r_{h2}, \dots, r_{hn})$ is the h^{th} pattern, and representing center point of HS m_j^k as $C_j^k = (c_{j1}^k, c_{j2}^k, \dots, c_{jn}^k)$, the membership function of the HS node m_j^k is defined as,

$$m_j^k(R_h, C_j^k, \zeta_j^k) = 1 - f(l, \zeta_j^k), \tag{5}$$

where $f(\cdot)$ is three-parameter ramp threshold function defined as,

$$f(l, \zeta_j^k, \nu) = \begin{cases} 0 & \text{if } 0 \leq l \leq \zeta_j^k \\ \nu & \text{if } \zeta_j^k < l \leq 1 \\ 1 & \text{if } l > 1 \end{cases} \tag{6}$$

and the argument l is defined as,

$$l = \left(\sum_{i=1}^n (c_{ji}^k - r_{hi})^2 \right)^{1/2} \tag{7}$$

The membership function returns $m_j^k = \nu$, if HS includes the pattern R_h . The sensitivity parameter ν , $0 < \nu \leq 1$, administers how fast the membership value decreases outside the HS, as the distance between R_h and C_j^k increases.

After training, the performance of MFHSNN is tested using four-layer feed forward neural network architecture as shown in Figure 5. The first two layers are constructed during training. The third layer uses four MAX Fuzzy Neurons (FNs), one for each module. The output of k^{th} module, n^k , is calculated as,

$$n^k = \max_{j=1}^{q^k} m_j^k \quad \text{for } k = 1, 2, \dots \tag{8}$$

where,

q^k represents number of HSs in k^{th} module created in training phase.

Thus, output of third layer gives fuzzy decision and the output n^k indicates the degree of membership of the input pattern to the class k . The fourth layer contains COMP-FNs. Finally, each F_C node delivers non-fuzzy output which is described as,

$$c^k = \begin{cases} 0 & \text{if } n^k < T \\ 1 & \text{if } n^k = T \end{cases} \quad \text{for } k = 1 \text{ to } 4 \tag{9}$$

where,

$$T = \max(n^k), \quad \text{for } k = 1 \text{ to } 4$$

Learning Algorithm

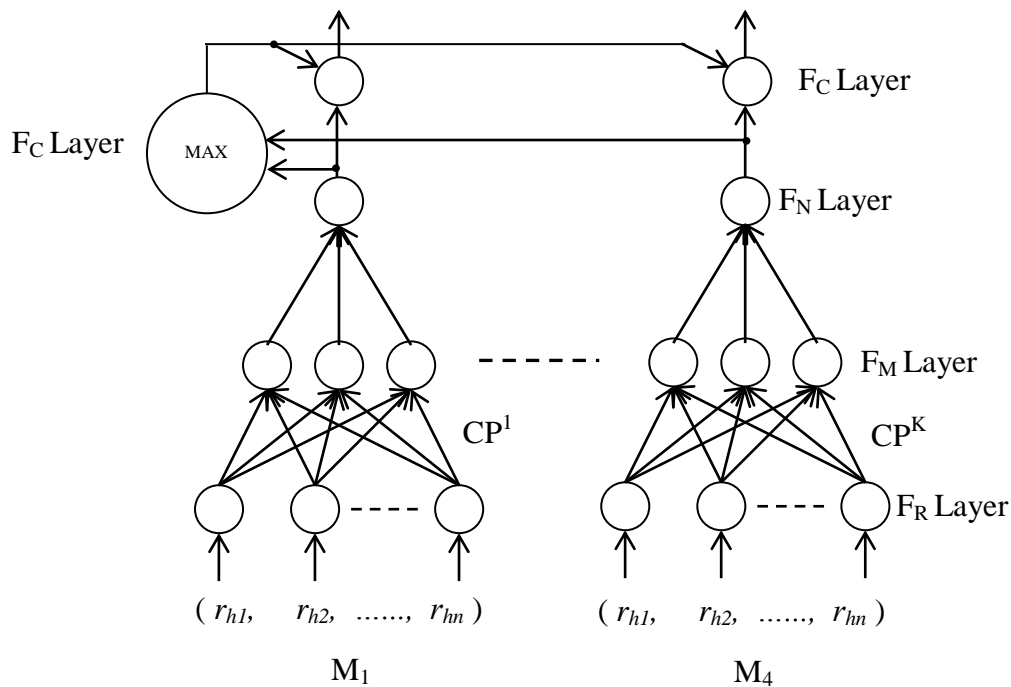
The training set consists of a set of ordered pairs (x_i, c_i) , where x_i is the input pattern and c_i is the index of one of the classes. The learning algorithm of MFHSNN composed of two steps.

Initialization

All the four modules are initialized by creating a HS in each, with a first pattern belonging to the class of the module. In this state, the network has four modules. Each module contains one HS having radius equal to zero and a center point initialized with the pattern of corresponding class.

Training

After the initialization, actual training begins. Class k input pattern is applied to k^{th} module only and then fuzzy membership of the input pattern with all the HSs within that module is calculated. Then one of the two cases that are described below can happen.



Figure(5): Architecture of MFHSNN in testing phase [1].

Case I: Accommodation by expansion of HS

Each HS has maximum limit on its radius denoted by the parameter λ . The pattern is included in the existing HS only if radius of that HS after expansion is less than or equal to λ ; as stated in (10). The HS is expanded to include the input pattern by modifying its radius if the criterion stated in (10) is satisfied. This is described by following two steps.

Step 1: Determine using (5), whether the pattern R_h is contained by any one of the existing HSs. With inclusion of R_h , the remaining steps in the training process are skipped and the training continues with the next training pair.

Step 2: If the pattern R_h falls outside the HS, then the HS is expanded to include pattern if the expansion criterion is met. For the HS r to include R_h ,

$$\left(\sum_{i=1}^n (c_{ji}^k - r_{hi})^2\right)^{1/2} \leq \lambda$$

(10)

If the expansion criterion is satisfied then the pattern R_h is included as,

$$c_j^{k, new} = \left(\sum_{i=1}^n (c_{ji}^k - r_{hi})^2\right)^{1/2}$$

(11)

Case II: Accommodation by creation of new HS

If case I fails, then to include the input pattern, a new HS is created as,

$$c_{new}^k = R_h \text{ and } z_{new}^k = 0$$

(12)

RESULTS AND DISCUSSIONS

In this work, we have measured bio-impedance of diseased and normal skin using developed skin electrode and Analog Devices board AD5933EBZ. The skin impedance was measured at 20 kHz and 500 kHz for various skin diseases, namely facial melanoses, acne vulgaris, folliculitis and tineacorporis. The impedance of normal skin adjacent to diseased skin was also measured at 20 kHz and 500 kHz. The impedance measurements showed overlapping readings for different diseases so that various indices, MIX, PIX, IMIX and RIX, computed based on impedance readings could be a mechanism for differentiation between the tissues of various diseases. Values of the indices have been computed for facial melanoses, acne vulgaris, folliculitis and tineacorporis. The indices were also computed for normal skin. The box and whisker plot has been used to exhibit the statistical variations in the measured dataset for various diseases. The mean and standard deviation were computed for various indices of diseased and normal skin. In case of facial melanoses, acne vulgaris, folliculitis and tineacorporis, the values of MIX was observed to be significantly lower than that of normal skin. Significant differences were observed between diseased and normal skin for IMIX values of facial melanoses and acne vulgaris. Few significant differences were observed in IMIX values of diseased and normal skin of folliculitis and tineacorporis. It has been observed that MIX, IMIX and PIX have shown statistically significant differences between diseased and normal skin for all the four said diseases based on Wilcoxon signed rank test. Excepting the case of folliculitis disease, RIX also shows statistically significant differences. Results comparing diseased skin of facial melanoses, acne vulgaris, folliculitis and tineacorporis, with normal skin, were similar to the state-of-the-art results reported for BCC lesions.

Further, we have classified facial melanoses, acne vulgaris, folliculitis and tineacorporis using MFHSNN and implemented on MATLAB platform. The database contains 108 patterns of 4 classes. Class 1 refers to 24 subjects of facial melanoses, Class 2 refers to 29 subjects of acne vulgaris, Class 3 refers to 37 subjects of folliculitis and Class 4 refers to 18 subjects of tineacorporis. All the classes were not linearly separable from each other. Feature vector is 13-dimensional, excluding class label, and has been used as input for FR Layer. For recognition purpose, set I and II were prepared from the database by randomly selecting 10 patterns in each class to form set I and remaining patterns of all the classes forms set II. When MFHSNN was trained with $\lambda = 0.01$ with set I, it has created 26 HSs and recognized 59 patterns out of 68 patterns in set II. The performance of MFHSNN for classifying the skin diseases has been observed for various skin diseases during testing phase. Out of 14 subjects of facial melanoses, 13 were correctly classified and 1 misclassified as folliculitis. Thus, the classification accuracy for facial melanoses was 92.86%. In case of acne vulgaris, out of 19 subjects, 17 were correctly classified; 1 misclassified as facial melanoses and 1 misclassified as tineacorporis. Hence, classification accuracy was 89.47% for acne vulgaris. In case of folliculitis, with 27 test subjects, 24 were correctly classified; 1 misclassified as facial melanoses and 2 as acne vulgaris. So, classification accuracy for folliculitis was 88.89%. For tineacorporis, out of 8 test subjects, 5 were correctly classified; 1 misclassified as facial melanoses, 1 as acne vulgaris and 1 as folliculitis. Hence, classification accuracy for tineacorporis was 62.5%. The overall classification accuracy for the for skin diseases was found to be 83.43%. The timing analysis of MFHSNN was also measured using these features. It was found that to get 100% recognition rate for set I, the training time required was 62.57 seconds at $\lambda = 0.01$, and number of HSs created were 26. The training of MFHSNN was required only once, hence the training time does not matter. The recall time per pattern was

found to be 0.163 seconds. It is clear that the MFHSNN gives better recognition rate with the less number of created HSs and is computationally efficient. The MFHSNN learns patterns faster because of its ability to create/expand HSs without any overlap test and its removal. Thus, one can add the new patterns on fly and the proposed system can be implemented for online voluminous dataset for classification of the skin diseases.

REFERENCES

- [1] P. M. Patil, U. Kulkarni and T. Sontakke, "Modular fuzzy hypersphere neural network," in IEEE International Conference on Fuzzy Systems (FUZZ), 2003, pp. 232-236.
- [2] P. Aberg, I. Nicander, J. Hansson, P. Geladi, U. Holmgren and S. Ollmar, "Skin Cancer Identification Using Multifrequency Electrical Impedance - A Potential Screening Tool," IEEE Transactions on Biomedical Engineering, vol. 51, no. 12, pp. 2097-2102, Dec. 2004.
- [3] I. Nicander, S. Ollmar, A. Eek, B. Lundh, R. Ozell and L. Emtestam, "Correlation of impedance response patterns to histological findings in irritant skin reactions induced by various surfactants," British Journal of Dermatology, vol. 134, pp. 221-228, 1996.
- [4] L. Emtestam, I. Nicander, M. Stenstrom and S. Ollmar, "Electrical Impedance of Nodular Basal Cell Carcinoma: A Pilot Study," Dermatology, vol. 197, pp. 313-316, Apr. 1998.
- [5] D. Beetner, S. Kapoor, S. Manjunath, X. Zhou and W. Stoecker, "Differentiation Among Basal Cell Carcinoma, Benign Lesions, and Normal Skin Using Electric Impedance," IEEE Transactions On Biomedical Engineering, vol. 50, no. 8, Aug. 2003.
- [6] T. Uchiyama, S. Ishigame, J. Niitsuma, Y. Aikawa and Y. Ohta, "Multi-frequency bioelectrical impedance analysis of skin rubor with two-electrode technique," Journal of Tissue Viability, vol. 17, no. 4, pp. 110-114, Nov. 2008.
- [7] S. Koppa, V. Savolainen and J. Hyttinen, "Modelling Approach for Assessment of Electrode Configuration and Placement in Bioimpedance Measurements of Skin Irritation," in European Conference of the International Federation for Medical and Biological Engineering (IFMBE), 2011, vol. 37, pp. 1238-1241.
- [8] H. Kwan and Y. Cai, "A fuzzy neural network and its applications to pattern recognition," IEEE Transactions on fuzzy systems, vol. 2, no. 3, pp. 185-192, 1994.
- [9] U. Kulkarni and T. Sontakke, "Modified fuzzy neural network classifier for pattern recognition," All India seminar on recent trends in computer communication networks (CCN), I.I.T. Roorkee, 2001, pp. 69-75.
- [10] P. Patil, U. Kulkarni and T. Sontakke, "Performance evaluation of Fuzzy Neural Network with various aggregation operators," in International Conference on Neural Information Processing (ICONIP), Singapore, 2002, vol. 4, pp. 1744-1748.
- [11] P. Patil, U. Kulkarni and T. Sontakke, "General Fuzzy Hyperline Segment Neural Network," in IEEE International Conference on Systems, Man and Cybernetics (SMC), Hammamet, Tunisia, 2002.
- [12] N. Khanna and S. Rasool, "Facial melanoses: Indian perspective," Indian Journal of Dermatology, Venereology and Leprology, vol. 77, no. 5, pp. 552-564, Oct. 2011.
- [13] P. Durai and D. Nair, "Acne vulgaris and quality of life among young adults in South India," Indian Journal of Dermatology, vol. 60, no. 1, pp. 33-40, Feb. 2015.
- [14] N. Stollery, "Skin infections," Practitioner, vol. 258, no. 1770, pp. 32-33, Apr. 2014.
- [15] A. Sahoo and R. Mahajan, "Management of tineacorporis, tineacruris, and tineapedis: A comprehensive review," Indian Dermatol Online Journal, vol. 7, no. 2, pp. 77-86, Apr. 2016.
- [16] Analog Devices. (2007). www.analog.com: www.analog.com/media/en/technical-documentation/user-guides/UG-364.pdf.
- [17] Cypress Semiconductor Corporation. (2015, Jan). [www.cypress.com: http://www.cypress.com/search/all/CY7C68013A](http://www.cypress.com: www.cypress.com/search/all/CY7C68013A).